Molecular hyperfine parameters in the $1\ ^3\Sigma_u^+$ and $1\ ^3\Sigma_g^+$ states of Li_2, Na_2, K_2 and Rb_2

Marius Lysebo

Department of Civil Engineering and Energy Technology,

Oslo and Akershus University College of Applied Sciences, 0130 Oslo, Norway

Leif Veseth

Department of Physics, University of Oslo, 0316 Oslo, Norway

(Dated: April 22, 2013)

Abstract

Magnetic hyperfine parameters have been computed for the $1\ ^3\Sigma_u^+$ and $1\ ^3\Sigma_g^+$ states of Li_2, Na_2, K_2 and Rb_2. The parameters were computed with MCSCF wavefunctions and the calculations were repeated for a series of internuclear distances. The results are compared with a recent observation of the hyperfine structure in Rb_2, and to the atomic hyperfine parameters. The available empirical data are reproduced with high accuracy. For the present systems the molecular hyperfine parameters are largely determined by the corresponding atomic hyperfine interactions. The computed molecular parameters at the dissociation limit deviate at most 11 % from the experimentally determined atomic ones.

I. INTRODUCTION

During the last two decades there has been considerable interest in the alkali dimers. At present these systems are subject to intense experimental research. The observed spectra reveal a rather complex hyperfine structure, and tend to be hard to interpret without the aid of theoretical predictions of the molecular hyperfine parameters. To the best of our knowledge, no *ab initio* study of the triplet state hyperfine parameters have appeared.

In general there seems to be rather few theoretical studies of the molecular hyperfine parameters. The first to study these parameters were Frosch and Foley [1], sixty years ago. Since then, many articles on the subject have been published, however, with a main focus on experimental work. Aldegunde *et al.* have published a series of papers [2, 3], based on density functional theory, exploring the singlet state hyperfine structure of the alkali dimers. Many hydrids and radicals [4–10] are also rather well studied. Previous theoretical studies are based on a variety of quantum chemistry methods. A more extensive, although not complete overview is given by Fitzpatrick *et al.* [11].

Ultracold alkali atoms have been used extensively in experiments over the last two decades. It has become standard practice to form cold dimers by the photoassociation technique, or by utilizing Feshbach resonances. These experiments populate the highly excited vibrational levels of the $1\ ^3\Sigma_u^+$ states. In the analysis of the experimental results it is standard to adopt the atomic hyperfine structure at the dissociation limit, without recourse to the actual molecular character of the system. The motivation for such a treatment is the large internuclear separations combined with the low binding energy.

For the lower lying vibrational levels it may in particular be insufficient to describe the hyperfine interaction only at the atomic level. In the present work we compute the molecular hyperfine parameters as a function of the internuclear distance. The hyperfine parameters in any vibrational level may then be obtained from our results, by averaging over the corresponding vibrational wave function.

A recent experimental investigation [12] revealed the hyperfine structure in the excited $1\ ^3\Sigma_g^+$ state of Rb_2 . This fact motivated us to carry out an extensive *ab initio* study of the hyperfine structure of this state as well. The $1\ ^3\Sigma_g^+$ state is a real molecular state, holding a large number of bound vibrational states, in contrast to the very shallow $1\ ^3\Sigma_u^+$ state.

We have chosen to focus on the alkali dimers Li_2, Na_2, K_2 and Rb_2. To continue further

down the first row of the periodic table seems difficult. Relativistic corrections are not included in the present work and they tend to be important for the heavier elements. In fact, it may be questionable to ignore such effects even for Rb_2.

To compute molecular hyperfine parameters is a very delicate matter. Most, if not all, of the previous theoretical studies reach the same conclusion. None the less, in the present work we want to make an effort to present *ab initio* results with a reasonable accuracy, which should be helpful for the interpretation of the complex observed spectra.

The spectra of the heavy alkali dimers are in particular hard to understand as the hyperfine splitting tend to be of the same size as the distance between the rotational levels. The molecular hyperfine parameters are somewhat unpredictable and non-intuitive, hence, even a rough estimate may prove useful. We will also attempt to give a few clues on how to perform a straightforward calculation of the hyperfine parameters with rather simple measures. This may be helpful for others working with the various electronic states of the alkali dimers.

The first section briefly reviews the theoretical approach. We devote a subsection to the connection between the atomic and the molecular hyperfine parameters, as this connection is very useful to test and evaluate the results. Section III A discusses the choice of basis sets. Our philosophy is to use standard basis set families where possible. The post-Hartree-Fock methods are briefly commented upon before we present the results. Finally, we discuss the expected accuracy of the results.

Throughout this paper atomic units are used unless otherwise stated.

II. THEORY

The general molecular hyperfine Hamiltonian is given in [4]. In the present paper we consider Σ-states, and only interactions that depend on the electronic spin are of interest. We will only be concerned with first-order hyperfine parameters, and only matrix elements diagonal in the quantum number Λ and S need to be considered. Starting from the microscopic

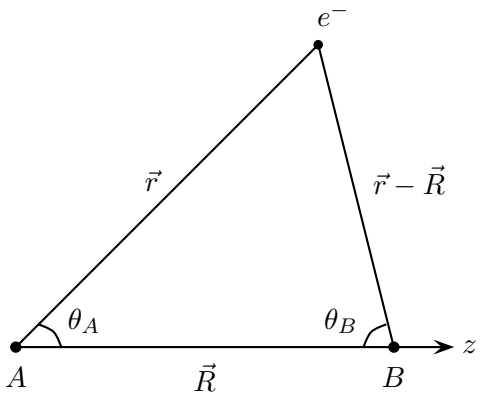

FIG. 1: Definition of symbols. A and B are the positions of the nuclei and $\vec{R}$ is the internuclear vector. The origin is at the position of nucleus A and the z-axis is along the internuclear axis.

hyperfine Hamiltonian, two molecular hyperfine parameters are defined [13]

$$b_F = \frac{16\pi}{3} g_I \mu_0 \mu_N \frac{1}{\Sigma} \left\langle qS\Sigma \left| \sum_{i=1}^{N} s_{iz} \delta(\mathbf{r}_i) \right| qS\Sigma \right\rangle, \tag{1}$$

$$c = 3 g_I \mu_0 \mu_N \frac{1}{\Sigma} \left\langle qS\Sigma \left| \sum_{i=1}^{N} \frac{3\cos^2\theta_A - 1}{|\vec{r_i}|^3} s_{iz} \right| qS\Sigma \right\rangle. \tag{2}$$

The summations are over the N electrons. The nuclear g factor is denoted g_I, and μ_N is the nuclear magneton. The angles θ_A and θ_B, together with the vectors $\vec{r}$ and $\vec{R}$ are defined in Fig. 1.

The molecular electronic state $|qS\Sigma\rangle$ ($\Lambda = 0$) is written as a linear combination of Slater determinants $|\Phi_i\rangle$

$$|qS\Sigma\rangle = \sum_i c_i |\Phi_i\rangle. \tag{3}$$

The Slater determinants are composed of molecular spin states $|\psi_i\rangle$. The matrix elements in Eqs. (1) and (2) are reduced to matrix elements involving the molecular spin orbitals (MOs) $\psi_i(r) = \langle r|\psi_i\rangle$, by the Slater-Condon rules for one-body operators.

The MOs are constructed from Gaussian functions χ, centered on one of the nuclei

$$\psi_i(\vec{r}) = \sum_k c_{ik} \chi_k(\vec{r}) + \sum_j c_{ij} \chi_j(\vec{r} - \vec{R}). \tag{4}$$

The basis functions employed are contracted Gaussian-type orbitals (GTOs)

$$\chi_i(\vec{r}) = \sum_{j=1}^{k} d_{ij}\phi_j(\vec{r},\alpha), \tag{5}$$

where d_{ij} are expansion coefficients. The general form of a GTO in atom-centered Cartesian coordinates is [14]

$$\phi(\vec{r},\alpha) = Nx^i y^j z^k e^{-\alpha(x^2+y^2+z^2)}, \tag{6}$$

where N is a normalization constant that depends on i, j, k and α.

To obtain the necessary matrix elements we need to solve the integrals

$$I_{kj} = \int \chi_k(\vec{r}) f(\vec{r}) \chi_j(\vec{r}-\vec{R})\ \mathrm{d}\vec{r}, \tag{7}$$

where $f(\vec{r})$ is one of the hyperfine operators from Eqs. (1) or (2). The Gaussian functions χ_k and χ_j in Eq. (7) relate to two different centers A and B. The origin coincides with the position of nucleus A and

$$|\vec{r}-\vec{R}|^2 = |\vec{r}|^2 + |\vec{R}|^2 - 2|\vec{R}|r_z, \tag{8}$$

and

$$(\vec{r}-\vec{R})_x = r_x, \qquad (\vec{r}-\vec{R})_y = r_y, \qquad (\vec{r}-\vec{R})_z = R - r_z. \tag{9}$$

The two-center integral (7) can now be expressed as a single center integral

$$I_{kj} = \int \chi_k(\vec{r}) f(\vec{r}) \chi_j(\vec{r}-\vec{R}) r^2 \sin\theta_A\ \mathrm{d}r\mathrm{d}\theta_A\mathrm{d}\phi_A. \tag{10}$$

We evaluate these integrals numerically with an adaptive Simpson quadrature method.

A. Hyperfine parameters in the atomic limit

The hyperfine structure in the alkali atoms have been observed in many experiments (see e.g. [15]), and accurate atomic hyperfine parameters are available. In the limit $R \to \infty$ the molecular hyperfine parameters tend to the corresponding atomic parameters. However, it is not obvious how the molecular hyperfine parameters relate to the corresponding atomic ones in this limit.

To make the connection clear, let us expand the molecular electronic states in terms of atomic states $|\lambda_i S_i M_{S_i}\rangle$. The electron spin quantum numbers are in the present study limited to the values $S_1 = S_2 = \frac{1}{2}$. λ is a label which identifies different electronic states. The quantum number M_S refers to the component of the electronic spin vector along the molecular axis.

The molecular electronic states are simultaneous eigenstates of the $\mathbf{S}^2$ operator with quantum number S, and of the orbital and spin angular momentum components L_z and S_z along the molecular axis. The symmetry operations σ_v and i classify the molecular states. σ_v denotes a reflection of the molecule fixed electronic coordinates in a plane containing the molecular axis, and i refers to an inversion of the electronic coordinates through the midpoint between the nuclei (g-u symmetry). The molecular states must also obey the Pauli exclusion principle. These requirements need to be incorporated in the atomic state expansion.

The symmetry operation σ_v mixes the different orbital and spin angular momentum components in a case (a) basis, according to [16]

$$\sigma_v|q\Lambda S\Sigma\rangle = (-1)^s|q - \Lambda S - \Sigma\rangle. \tag{11}$$

Λ and Σ are the quantum numbers corresponding to L_z and S_z respectively. In Σ-states ($\Lambda = 0$), $s = 0$ corresponds to Σ^+, and $s = 1$ corresponds to Σ^-. The labels Σ^+ and Σ^- refer to the symmetry of the orbital electronic part of the wave function, that may be inferred from the atomic eigenstates according to the Wigner-Witmer rules [17].

In a case (a) basis it is not possible to construct simultaneous eigenstates of the σ_v symmetry operator, and of the orbital and spin angular momentum components. The definitions of b_F (Eq. (1)) and c (Eq. (2)) require us to work with eigenstates of the orbital and angular momentum operators. Hence, we will be working with the case (a) states $|q\Lambda S\Sigma\rangle$. The electronic states relevant for the present work are both Σ^+-states.

Let us first consider the $1\ ^3\Sigma_u^+$ state vector $|qS\Lambda\Sigma\rangle$ and expand it in terms of atomic eigenstates. This molecular state dissociates into two identical ^{2}S-states. To make the derivation as simple as possible we consider the state

$$|q\Lambda S, \Sigma = 1\rangle_u = \left|\lambda_1, M_{S_1} = \frac{1}{2}\right\rangle_A \left|\lambda_2, M_{S_2} = \frac{1}{2}\right\rangle_B. \tag{12}$$

The two atoms are identical and $\lambda_1 = \lambda_2$. It can be shown that the state in Eq. (12) is an eigenstate of the inversion operator i, with eigenvalue -1, corresponding to the label u.

In the limit $R \to \infty$, the Fermi contact parameter (Eq. (1)) is obtained in terms of atomic eigenstates using Eq. (12)

$$b_F = \frac{16\pi}{3} g_I \mu_0 \mu_N \frac{1}{\Sigma} \left\langle \lambda_1, M_{S_1} \middle| \sum_{i=1}^{N} s_{iz} \delta(\mathbf{r}_i) \middle| \lambda_1, M_{S_1} \right\rangle \left\langle \lambda_2 M_{S_2} \middle| \lambda_2 M_{S_2} \right\rangle. \tag{13}$$

The Fermi contact parameter b_F in Eq. (13) is recognised as half the atomic Fermi contact term b_F^{atm}. The factor of $\frac{1}{2}$ stems from $\frac{1}{\Sigma}$, which is 1 for the molecular state and 2 for the atomic state. Hence, the conclusion is

$$b_F = \frac{1}{2} b_F^{atm}, \tag{14}$$

in the limit of two atomic ^{2}S-states. The anisotropic c-parameter does not exist for S atoms, and approaches zero when $R \to \infty$.

The 1 $^3\Sigma_g^+$ state dissociates to the ^{2}S+^{2}P atomic limit. The two atoms are not in identical states, and two terms are needed to construct eigenstates of the electronic inversion operator i in the limit $R \to \infty$. We once more consider states with quantum number $\Sigma = 1$, and the linear combination below yields an eigenstate for i with eigenvalue +1, i.e. a g-state. Hence, we have for the 1 $^3\Sigma_g^+$ state:

$$|q\Lambda S, \Sigma = 1\rangle_g = \frac{1}{\sqrt{2}} \left(\left| \lambda_1, M_{S_1} = \frac{1}{2} \right\rangle_A \left| \lambda_2, M_{S_2} = \frac{1}{2} \right\rangle_B - \left| \lambda_2, M_{S_2} = \frac{1}{2} \right\rangle_A \left| \lambda_1, M_{S_1} = \frac{1}{2} \right\rangle_B \right). \tag{15}$$

The molecular Fermi contact parameter can now be written in terms of the atomic eigenstates using Eq. (15). The result is

$$b_F = \frac{16\pi}{3} g_I \mu_0 \mu_N \frac{1}{\Sigma} \frac{1}{2} \left[\left\langle \lambda_1 M_{S_1} \middle| \sum_{i=1}^{N} s_{iz} \delta(\mathbf{r}_i) \middle| \lambda_1 M_{S_1} \right\rangle + \left\langle \lambda_2 M_{S_2} \middle| \sum_{i=1}^{N} s_{iz} \delta(\mathbf{r}_i) \middle| \lambda_2 M_{S_2} \right\rangle \right]. \tag{16}$$

One of the two labels λ_1 or λ_2 refers to a ^{2}P state with zero electron density at the nucleus. Hence, only one of the two terms in Eq. (16) will be non-zero, and

$$b_F = \frac{1}{4} b_F^{atm} \tag{17}$$

at the ^{2}S +^{2} P dissociation limit. This conclusion actually holds for all $^3\Sigma$-states at this dissociation limit, irrespective of their g-u symmetry.

Finally, the anisotropic hyperfine parameter c is not zero due to the atom in the ^{2}P-state. However, the relationship between this parameter and the atomic hyperfine parameter(s)

seems to be somewhat involved. At the dissociation limit the molecular electronic Π- and Σ-states interact with matrix elements $\langle \Pi | H_{hf} | \Sigma \rangle \neq 0$, where H_{hf} is the hyperfine Hamiltonian defined in Eq. (4) in [4]. We recall that for Π-states there are extra molecular hyperfine parameters that need to be considered. Together with the anisotropic hyperfine parameter c these extra parameters reproduce the atomic hyperfine splitting at the dissociation limit. However, the numerical values for the c parameters are rather small, and we have not perused this problem any further.

III. COMPUTATIONAL METHODS

The molecular electronic states $|qS\Sigma\rangle$ are obtained from the quantum chemistry package GAMESS [18, 19], with input to our own code that computes the hyperfine parameters from Eqs. (1) and (2), as outlined in Sec. II.

For the ground triplet state our initial investigation was based on restricted open-shell Hartree-Fock (ROHF) wavefunctions, and gave a rough estimate for the hyperfine parameters. Later we combined the ROHF with configuration interaction (CI) as the post Hartree-Fock method. Compared to the ROHF results the CI calculations add minor corrections to the results. Our final approach was to use Multi-configurational self-consistent field (MCSCF) wavefunctions to increase the accuracy of the results. We will give more specific results in subsection III B, here we only remark that MCSCF wavefunctions typically yield an increase in the variation of the hyperfine parameters with R.

A. Basis sets

The basis functions χ are of great importance for the molecular hyperfine parameters. For the alkalis it is certainly far more important than any post-Hartree-Fock method we could choose.

Although many good and flexible basis sets have been developed, calculation of different molecular properties may require different basis sets. For the present investigation we expect the Fermi contact term b_F to be the most interesting. From the definition in Eq. (1) we immediately see that this parameter depends dramatically on the wavefunction at the nucleus. Most Gaussian expansions such as Eq. (5) are determined (d and α) by minimization

of the total HF energy. Although this may provide an excellent description of the electronic states, the geometry and other properties, we find the corresponding molecular hyperfine parameters to be in rather poor agreement with observations.

The results for the alkalis are improved considerably using Slater orbitals (STOs). The alkalis have a simple and hydrogen-like electronic structure that seems to make the physical Slater orbitals preferable. We will therefore primarily use the minimal STO-kG basis of Hehre, Stewart and Pople [20], where k Gaussian functions (cf. Eq. (5)) are used to represent a single Slater orbital. The expansion coefficients in Eq. (5) are then obtained by a least-squares procedure to best represent the STOs. The basis sets are augmented with two d-functions through the option NDFUNC in GAMESS.

To find a suitable basis set we use the Fermi contact parameter b_F at the atomic limit as a guide. Basis sets that do not reproduce the atomic hyperfine parameter with a relative error less than 10 % are excluded. It is important to model the atomic hyperfine interaction rather well in the alkalis. With the large internuclear separations the majority of the electron density present on one of the nuclei is from the electrons surrounding that nucleus.

Table I shows good agreement between the experimental atomic hyperfine parameters and the computed values with various STO-kG basis sets. More advanced basis sets, traditionally regarded as superior, perform rather poorly with respect to the hyperfine parameters. We do of course not dispute the fact that these simple STO-basis sets are inadequate for very accurate calculations of other properties. Therefore we can not expect to describe the electronic states in an accurate manner by such simple basis sets. Discrepancies in the equilibrium distances and dissociation energies must be expected, and are summarized in Table II.

The reader may well ask how the discrepancies in the potential curves influence the molecular hyperfine parameters. Numerical tests have shown that the parameters have a low sensitivity to the depth of the potential well, and a moderate sensitivity to the bond length. A remark of caution: This may not be true in general, but apply to the alkali dimers.

Accurate potential curves were computed using sophisticated basis set. However, the numerical values for the molecular hyperfine parameters were then seriously in error. Still, the functional form of $b_F(R)$, as well as the variation with R, were similar for many basis sets, including the STO-kG.

The upper right panel of Fig. 4 shows a comparison of the Fermi contact term b_F

Basis	^{6}Li	^{23}Na	^{39}Ka	^{87}Rb
experiment [15]	76.07	442.8	115.4	1708
STO-3G	80.32	263.4	109.3	894.3
STO-4G	95.89	336.6	152.9	1369
STO-5G	109.5	3.5	183.2	1753
STO-6G	119.2	427.7	173.2	NA
N21-3G	52.16	212.2	53.59	673.6
DZV	59.93	NA	71.89	NA
cc-pVDZ	52.34	305.8	NA	NA
STO/N21-own	NA	442.0	NA	NA

TABLE I: Computed values (ROHF) in MHz for the atomic Fermi contact term $b_F^{atm}/2$ with different basis sets. Colored cells highlight the preferred basis sets used in the present work. See the text and Appendix 1 for more information on the STO/N21-own basis set. (NA: Not available.)

	$1\ ^3\Sigma_u^+$		$1\ ^3\Sigma_g^+$	
	R_e (a.u.)	D_e (cm^{-1})	R_e (a.u.)	D_e (cm^{-1})
Li_2 [21, 22]	7.80 (8.05)	197 (334)	5.80 (5.86)	7000 (6700 − 7000)
Na_2 [23]	9.20 (9.62)	360 (174)	6.80 (7.14)	6300 (4700)
K_2 [24]	9.20 (10.84)	378 (232)	8.30 (8.99)	6700 (3778)
Rb_2[25]	12.4 (11.7)	100 (240)	9.50 (10.0)	4000* (3209)

TABLE II: : Comparison of some key parameters for the two electronic states relevant to the present work. The preferred basis sets (see Table I) can not give an accurate representation of the molecular potential curves. The numbers in parenthesis are from the cited works and should be compared to the values we have computed. The papers cited do not necessarily represent the most reliable curves. For some systems there are still significant discrepancies in the literature. *: Only an estimate. It is difficult to obtain a converged solution at large internuclear distances.

computed with two different basis sets. The results represented with a solid (blue) line are calculated with the STO/N21-own basis set, which reproduce the potential curve fairly well. The (cyan) circles, however, represent results obtained with the STO-6G basis set, which completely fails to reproduce the potential curve. The well depth is in fact overestimated by more than 10000 cm^{-1}. The differences in the computed hyperfine parameter are still rather small. Then, the opposite conclusion is also close at hand: Two basis sets with almost identical potential curves may yield very different hyperfine parameters.

In conclusion, we should require from the basis sets:

1. As $R \to \infty$ the atomic hyperfine splitting must be be reproduced.

2. A "reasonable" description of the potential curve.

With respect to requirement 2 our conclusion is that most emphasize should be put on predicting the equilibrium distance.

For Na_2 the STO basis set did not represent the electronic states in an adequate manner, i.e. requirement 2 was not met. A new basis set, labeled "STO/N21-own" was constructed, inspired by the STO-5G and N21 basis sets, modified to reproduce the atomic Fermi contact term. See appendix 1 for a detailed description.

B. Post-Hartree-Fock method

As already mentioned the MCSCF wavefunctions were obtained with the quantum chemistry package GAMESS. Table III presents a comparison between post-Hartree-Fock methods at the internuclear distance $R = 6.0$ a.u. for the triplet ground state of Li_2. The table shows the total energy and hyperfine parameters from only HF, from HF + CI and finally from a MCSCF calculation. The CI and MCSCF corrections are rather small for both the hyperfine parameters, however, with a dominant MCSCF correction.

The Fermi contact parameter is sensitive to the computational method, and with MCSCF there are always some noise or discontinuities in the $b_F(R)$ function. These are most often rather small ($\simeq 1-2$ % of b_F^{atm}), and were averaged out from the reported results.

For the lowest triplet states the CI step in the MCSCF calculation is based on the Ames Laboratory determinant full CI code (ALDET) [26]. This means full CI within the chosen active space [27]. The excited triplet states are similarly described by MCSCF wavefunctions,

$1\ ^3\Sigma_u^+$	E (a.u.)	b_F (MHz)	c (MHz)
ROHF	-14.62671	75.87	0.8778
CI	-0.002843	-0.3900	-0.0208
MCSCF	-0.003654	-4.770	0.2112

TABLE III: Contributions to the total energy and to the hyperfine parameters from Hartree-Fock, CI and MCSCF. The results are for $R = 6.0$ a.u. in the lowest triplet state of Li_2. The numerical values for CI and MCSCF are relative to the ROHF results.

but the CI step is provided by the graphical unitary group CSF (GUGA) [28]. For the excited states we specify second order CI, with all singly and doubly excited configurations from the reference included. We use the default orbital optimizer in GAMESS, labeled SOSCF [29].

In general the design of active spaces is a matter of great importance in MCSCF calculations. Below we briefly discuss the active spaces used in the present work. Admittingly, these choices are influenced by the available computational resources.

For Li_2 the number of electrons and orbitals are quite manageable, and all orbitals are part of the active space. The computational cost makes it necessary to select active orbitals for Na_2, K_2 and certainly for Rb_2.

Valence MCSCF calculations were performed for the lowest triplet state in Na_2, K_2 and Rb_2. The active spaces were defined as the valence MOs obtained from the atomic valence orbitals. With full valence active space a convergent solution could be obtained at most internuclear distances. The Fermi contact parameter attained unrealistic values at some internuclear distances. In particular for the lowest triplet state in Na_2. The reason is probably that the MCSCF wavefunction has converged to a false solution. Anyway, the electron density at the nuclei was not described in a satisfactory manner in those cases, and these values were identified and removed from the final results.

For K_2 we were unable to obtain a satisfactory converged solution at internuclear distances larger than 13.5 a.u.. As the variation with R is rather small in this region, we did not consider this as an important problem.

Rubidium tend to be preferred by experimentalists, however, it is difficult to perform reliable *ab initio* calculations for such a heavy element. A general problem met in the calculations for the $1\ ^3\Sigma_u^+$ state, was to obtain a properly converged MCSCF wavefunction.

At some internuclear distances the calculations did not converge at all. Sometimes this problem could be overcome by small adjustments of the internuclear distance. Despite that, at$R > 15$ a.u. the convergence remains poor. A potentially more severe problem was the tendency to converge to a false solution. This problem was also strongly dependent on R.

After removal of the results obtained from poor convergence and false solutions, we were left with a Fermi contact parameter that displayed some oscillatory behavior with R. These oscillations were averaged out by fitting the results to a higher order polynomial. The cause of these oscillations is, unfortunately, not clear. The problems are present only for the MCSCF procedure, and were isolated to the $1\ ^3\Sigma_u^+$ state. Changing the convergence criteria does have some effect, although it does not solve the problem. The calculations were repeated using ROHF and CI, and the results were compared to those obtained from the MCSCF wavefunction. The minimum of the $b_F(R)$ curve (see in the lower right panel of Fig. 2) is shifted upwards with approximately 100 MHz relative to the MCSCF results. Comparing results obtained with the MCSCF-method to those obtained with ROHF + CI, we see that this is a typical feature of the Fermi parameter, and we find similar tendencies also for the other alkalis.

The active spaces for the $1\ ^3\Sigma_g^+$ state calculations in Na_2, K_2 and Rb_2 consist of two singly occupied orbitals in addition to the valence orbitals. For certain combinations of system, state and internuclear distances, convergent results could not be obtained without including at least one additional doubly occupied orbital in the active space.

The calculations on Rb_2 remain challenging also for the $1\ ^3\Sigma_g^+$ state, and we could only obtain a convergent solution for $8.0 < R < 14$ a.u.. However, the oscillatory behavior that obscured the ground state calculations did not occur.

IV. RESULTS: HYPERFINE PARAMETERS FOR THE $1\ ^3\Sigma_u^+$ STATE

The method for computation of the hyperfine parameters is outlined in Sec. III. We recall that the hyperfine parameters depend only on the isotope through g_I, see Eqs. (1) and (2). Although we report the hyperfine parameters for a particular isotope, it is straightforward to convert the numerical values to a different isotope using the data in table IV.

Generally the "ground" triplet states in the alkali dimers are shallow, with depths less than 1000 cm^{-1}, and with large equilibrium internuclear distances (see Table II).

Isotope	g_I	I	Isotope	g_I	I	Isotope	g_I	I
^{6}Li	0.8221	1	^{39}K	0.2610	1.5	^{85}Rb	1.101	2.5
^{7}Li	2.171	1.5	^{40}K	−0.3245	4	^{87}Rb	1.834	1.5
^{23}Na	1.478	1.5	^{41}K	0.1432	1.5			

TABLE IV: The alkali isotopes relevant to the present work. The values for g_I can be used to transform the reported hyperfine parameters to other isotopes. (cf. Eqs. (1) and (2)). The magnetic moments used to obtain g_I are from [30].

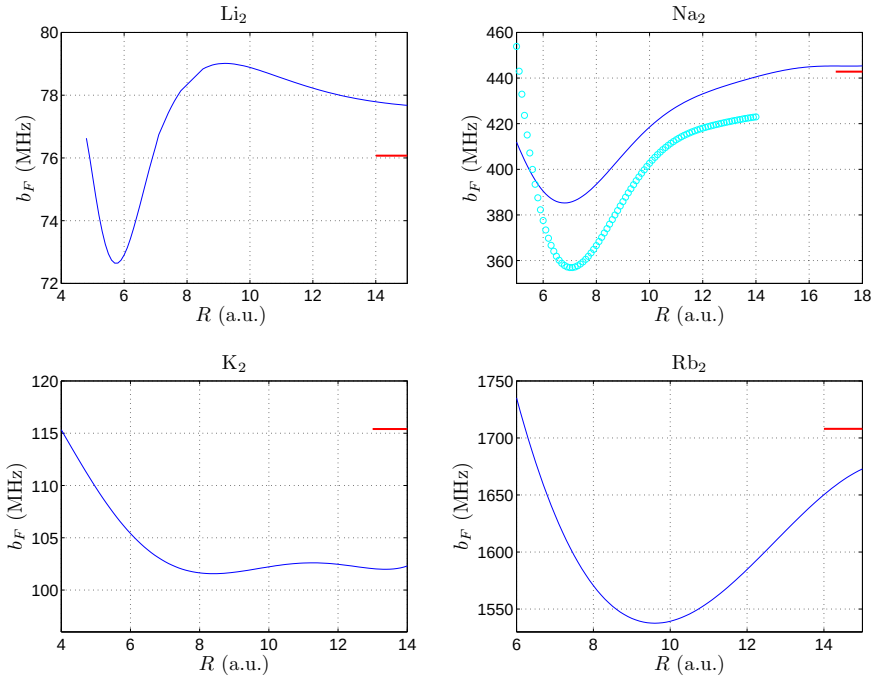

FIG. 2: The Fermi contact parameter $b_F(R)$ in the 1 $^3\Sigma_u^+$ electronic state of ^{6}Li$_2$,^{23} Na$_2$,^{39} K$_2$ and ^{87}Rb$_2$. The red horizontal lines show the corresponding empirical values for the atomic Fermi contact term $b_F^{atm}/2$. The (cyan) circles in the upper right panel shows results obtained with an alternative basis set. See the discussion in Sec. III A.

We have computed the Fermi contact parameter b_F as a function of the internuclear distance R. The results are displayed in Fig. 2. The horizontal red lines show empirical data at the atomic limit for comparison.

A general result is that the Fermi contact parameter increases rapidly at small inter-

nuclear distances, and approach a constant value at large distances. This constant should be compared with the well-known atomic parameters. The behaviour in the intermediate region is slightly different for the four systems studied in the present work. For potassium the variation with R is rather insignificant, whereas the results for rubidium are the most sensitive to variations in R.

We see from Fig. 2 that the computed contact parameters are generally not equal to the atomic values at large internuclear distances. The differences are partly inherited from the variations in the atomic values presented in Table I. There are also additional differences due to our finite upper value of R. Finally, the fact that finite basis sets are used leads to errors which are difficult to estimate. Comparisons with the atomic parameters yield an important indicator of the accuracy, and the relative errors are presented in Table V.

	Li_2 [%]	Na_2 [%]	K_2 [%]	Rb_2 [%]
$1\ ^3\Sigma_u^+$	2.1	< 1.0	11	2.1
$1\ ^3\Sigma_g^+$	1.9	< 1.0	11	< 1.0

TABLE V: Comparison of the computed molecular Fermi contact parameters with the empirical atomic Fermi contact parameters. The table presents relative errors at the maximum internuclear distances considered.

In potassium there is a rather large deviation ($\simeq$ 13 MHz) between the atomic and molecular parameter at $R = 13.0$ a.u. The main reason tend to be related to the basis set. The results suggest that the variation with R is very small for the contact parameter in potassium (cf. Fig. 2). Different combinations of basis sets and post Hartree-Fock methods yield similar consistent results. Thus, we believe that this slow variation reflects physical reality, although the atomic parameter is not well reproduced. More accurate results might be obtained by adjusting (increasing) the active space, however, such an increase generally made it difficult to obtain fully convergent solutions.

The equilibrium distances lie between $8.0 - 12$ a.u. for the $1\ ^3\Sigma_u^+$ state of the four dimers studied in the present work. The vibrational wavefunctions will have small amplitudes at the smallest internuclear distances. Thus, the rapid increase with R in this region is expected to make only a modest contribution to the vibrational dependency of the parameters. However,

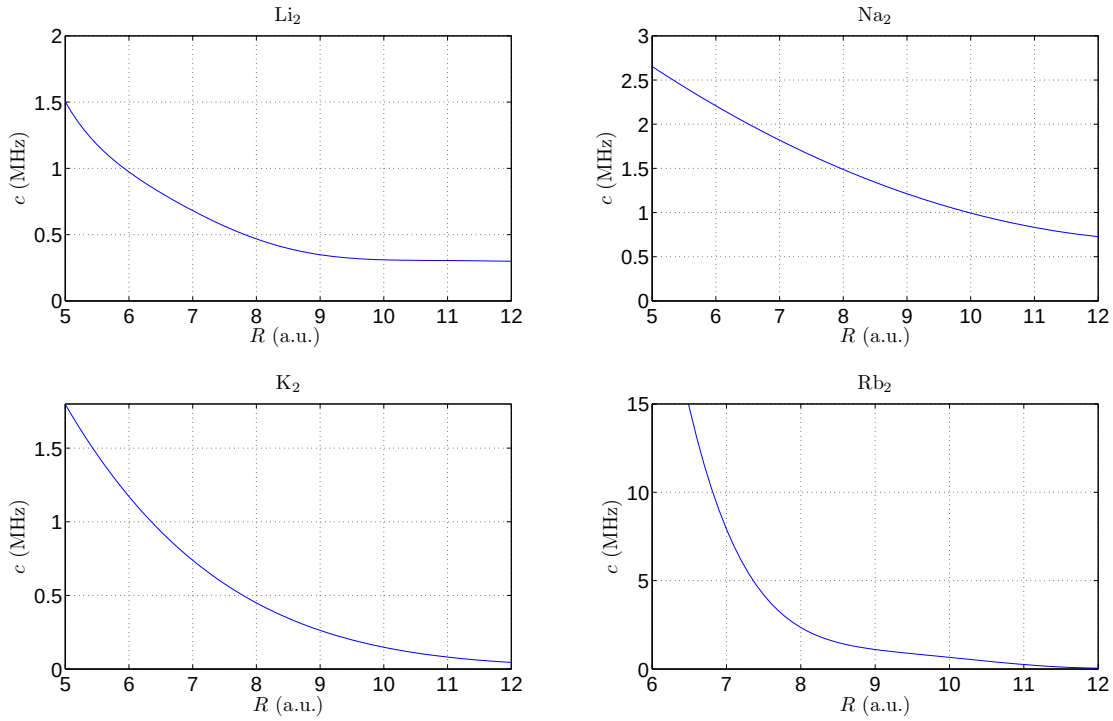

FIG. 3: The anisotropic magnetic hyperfine parameter c as a function of the internuclear distance R for the 1 $^3\Sigma_u^+$-state of ^{6}Li$_2$,^{23} Na$_2$,^{37} K$_2$ and ^{87}Rb$_2$.

in sodium the Fermi contact parameter increases with $20-30$ MHz from 10 a.u. to 20 a.u., and there may be a measurable vibrational dependency.

Finally, let us now turn to the anisotropic hyperfine parameter c. At the atomic limit the parameter vanishes. It falls off rapidly with R (see Eq. (2)), and is expected to be small, as confirmed by the results presented in Fig. 3. The numerical values are negligible compared to b_F for all systems investigated in the present work.

At this stage it is interesting to compare the results with those of earlier investigations. The present authors have previously reported computed values of the hyperfine parameters $b_F(R)$ and $c(R)$ for ^{6}Li$_2$ [13]. The values obtained for b_F at and around $R = 5$ a.u. differ slightly. The present result is 75.4 MHz at $R = 5.0$ a.u. with a minimal value of 72.7 a.u. at $R = 5.8$ a.u. The corresponding results from [13] are $b_F = 80$ MHz, and 76 MHz at $R = 5.0$ a.u. and 5.8 a.u. respectively. Comparison of the c parameter reveals excellent agreement.

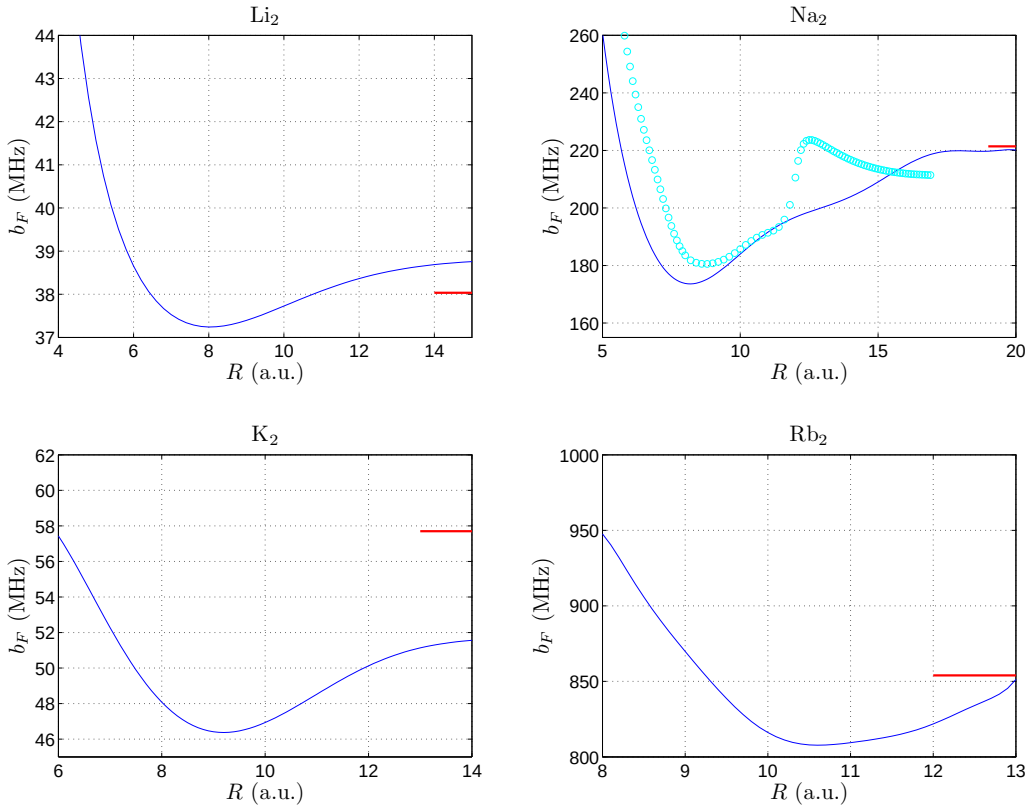

FIG. 4: The Fermi contact parameter b_F as a function of the internuclear distance R for the 1 $^3\Sigma_g^+$ electronic state of $^6Li_2$,$^{23}Na_2$,$^{39}K_2$ and $^{87}Rb_2$. The (cyan) circles in the upper right panel presents results with an alternative basis set. See the text in Sec. III A for a detailed description of the basis set, and Sec. V for a discussion of the results. The red horizontal lines show the corresponding empirical values for the atomic Fermi contact term.

V. RESULTS: HYPERFINE PARAMETERS FOR THE 1 $^3\Sigma_g^+$ STATE

This excited triplet state is for all the alkalies much more strongly bound than the lowest 1 $^3\Sigma_u^+$ state ($D_e = 3200 - 6000$ cm^{-1}). The computed hyperfine parameters for the excited states are presented as a function of the internuclear distance in Figs. 4 and 5.

The Fermi contact parameters b_F in the excited states are more sensitive to variations in R, and more dependent on the bond length. However, the R-dependence is limited to merely $10 - 20$ % of the atomic limit values, see Fig. 4.

As already mentioned in Sec. III, to find a suitable basis set for sodium represents a

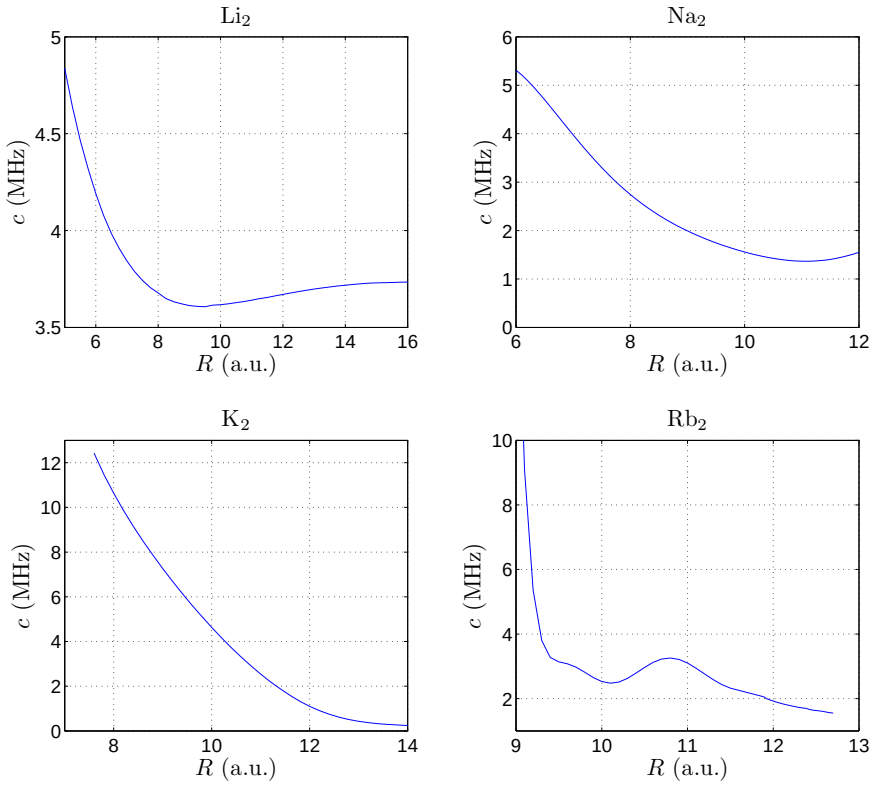

FIG. 5: The anisotropic magnetic hyperfine parameter c as a function of the internuclear distance R for the 1 $^3\Sigma_g^+$-state of ^{6}Li$_2$,^{23} Na$_2$,^{37} K$_2$ and ^{87}Rb$_2$.

special challenge. Results from a calculation with the STO6G basis set are included in Fig. 4 (cyan circles). The excited state is not well represented in this basis, in fact, the depth of the potential curve is overestimated by roughly 10000 cm^{-1}. Still, the results obtained with the two basis sets are quite similar, apart from the region at and around 13 a.u., as seen in the upper right panel of Fig. 4. We believe that this odd maximum is an artifact of the calculations, due to the inferior representation of the electronic state by the basis set.

The anisotropic hyperfine parameter c takes rather insignificant values also for the 1 $^3\Sigma_g^+$ states, see Fig. 5. It has, however, a strong dependence on R. The relative importance of the c parameter is largest in potassium, due to the small hyperfine splitting in the S-state K atom. For the other species, the Fermi contact parameter b_F is by far the most interesting. It is also worth noting that at large internuclear distances the c parameter do not go to zero at the S + P dissociation limit, but rather tend to a small value.

Overall, the shapes of the curves showing the anisotropic hyperfine parameter $c(R)$ are rather similar in Li_2, Na_2, K_2 and Rb_2. In rubidium there is a local maximum between $10 - 11$ a.u., unique to this system. There seems to be no good reason to believe that such a maximum reflects a physical reality.

An experimental study of the $1\ ^3\Sigma_g^+$ state has been carried out by Takekoshi *et al.* [12]. Based on the empirical data, the combination $b_F + \frac{2}{3}c$ was estimated to be 833 MHz [12] for $v = 10$. This is in good agreement with the results in the present work. At the relevant internuclear distances we find b_F to vary between $850 - 810$ MHz, whereas the value of c is less than 10 MHz. The function $b_F(R)$ would have to be averaged over the relevant vibrational wavefunction to make a complete comparison.

VI. AN EXAMPLE: THE $v = 0$ VIBRATIONAL LEVEL IN THE $1\ ^3\Sigma_g^+$ STATE OF Rb_2

The final step to reproduce observed quantities is to average the computed hyperfine parameters over the vibrational wave functions $\psi_v(r)$, e.g. for $b_F(R)$

$$b_F = \int_0^\infty \psi_v(r) b_F(R) \psi_v(r) dR. \tag{18}$$

As a specific example we will now compute the energy levels of the $v = 0$ vibrational level in the $1\ ^3\Sigma_g^+$ state of Rb_2. The necessary matrix elements are given in [12], together with the rotational constant B_e and the effective spin-spin splitting constant for this state. The Fermi contact term is strongly dominant, and we make the approximation of setting $c = 0$. In this way we obtain $b_F = 805$ MHz for $v = 0$.

The spin-spin interaction is rather strong, and splits the spectrum according to the quantum number $|\Omega| = |\Sigma + \Lambda| \in \{0, 1\}$. The energy levels are shown with the corresponding quantum numbers F and I in Fig. 6.

The hyperfine splitting is seen to be large, and comparable to that of the rotational levels. The spectrum might therefore be hard to interpret, as there is no regular rotational structure that can be easily identified. Clearly, no rotational quantum number can be associated with the individual levels.

Even if the computed values of the hyperfine parameters are not of experimental accuracy, their approximate values should represent a considerable aid in the interpretation of such

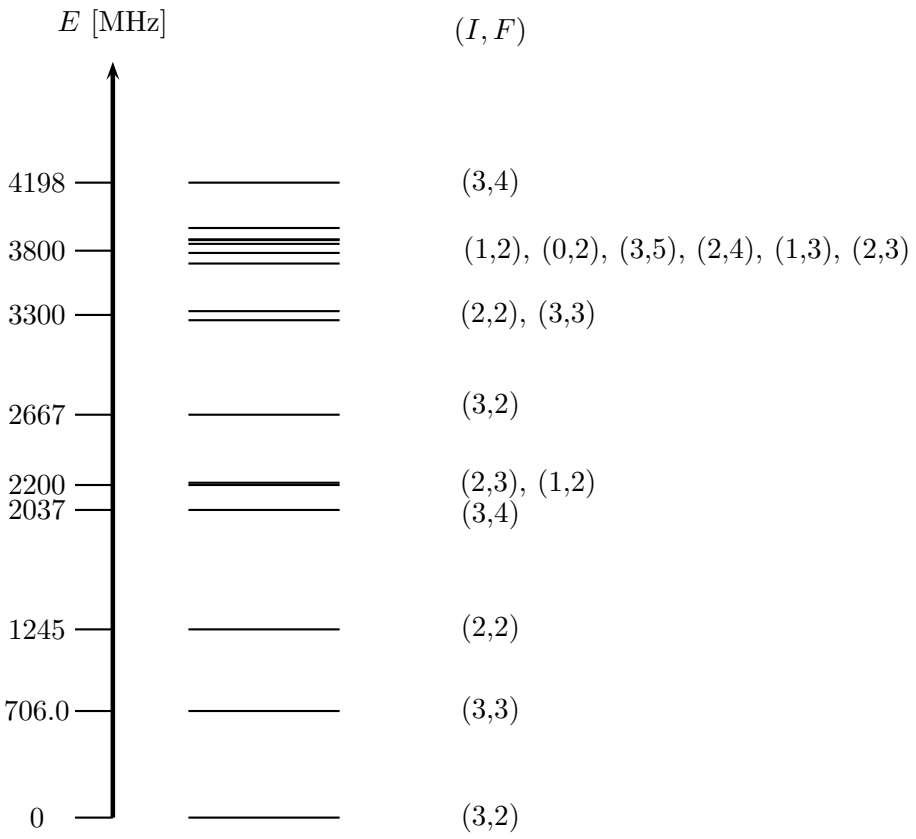

FIG. 6: The 16 lowest laying energy levels for $|\Omega| = 1$ and $v = 0$ in the $1\ ^3\Sigma_g^+$ state of Rb_2. The structure is rather irregular as the rotational and hyperfine splittings are of comparable size.

complex spectra.

VII. CONCLUDING REMARKS

For the dimers Li_2, Na_2, K_2 and Rb_2 we have shown that the computed molecular hyperfine parameters depend strongly on the basis set. This has been documented before in other atomic and molecular systems.

By working out the relationship between the atomic and the molecular hyperfine parameters, we were able to use the observed atomic parameters to evaluate the basis sets. It is also important to investigate how well a chosen basis set reproduces other basic molecular, like the bond length and depth. This is in particular exemplified by our results for the sodium

dimer. A compromise between these two aspects, mostly emphasising the properties of the atomic parameter, seems to be necessary to obtain a satisfactory basis set.

Using MCSCF wavefunctions, simple and carefully chosen basis sets, we have computed the magnetic hyperfine parameters for $^3\Sigma$ states of Li_2, Na_2, K_2 and Rb_2. The atomic values at the dissociation limit are reproduced within errors of 11 % or less. We believe that these discrepancies also yield good estimates of the accuracies of the computed molecular parameters. This assumption is furthermore supported by comparisons with observed molecular hyperfine parameters in Rb_2, and previous calculations on Li_2.

The results presented here suggest that the R-dependence of the molecular parameters merely amounts to $10 - 20$ % of the atomic values. The dependence is in particularly weak in Li_2 and K_2. In fact, in K_2 we find very little dependence of R at all. This could be an artifact of the calculations, but it has been a consistent feature of the results even with various basis sets and different post Hartree-Fock methods.

The computed minima in the parameter $b_F(R)$, at intermediate internuclear distances, tend to depend on the post Hartree-Fock method. The main source of errors still seems to be the basis sets, and their ability to accurately describe the electronic density at the nuclei. Relativistic effects are expected to be negligible for Li_2, but may be important for Rb_2, and thereby influence the accuracy for the heavier elements.

In addition to the magnetic hyperfine parameters b_F and c considered in the present work, there are a few more (subtle) parameters of a different kind. Electric quadrupole effects arise from the non-spherical distribution of the nuclear charges, and there is a coupling between the nuclear magnetic moments and the magnetic field generated by the rotation of the molecule (molecular spin-rotation coupling). Finally, there is also a spin-spin interaction that stems from the two nuclear spin magnetic moments of a dimer. The electric quadrupole effects may be of the same order of magnitude as the magnetic ones, but generally smaller. The other two effects mentioned above, yield contributions far below those from the dominant parameters b_F and c. Of the extra effects referred to above, only the electric quadrupole interaction has been considered in the present work. The relevant parameter can easily be computed once the anisotropic hyperfine parameter c is known, see [31]. However, our calculations show that the electric quadrupole interaction is weak. In $^{39}K_2$ it amounts to 30 % of the anisotropic hyperfine interaction, in the other dimers merely 10 % or less. Compared to the Fermi contact interaction the electric quadruple interaction is negligible.

s orbitals:		p orbitals:		l orbitals:		
exponent	coefficient	exponent	coefficient	exponent	s-coefficient	p-coefficient
9993.2	0.0019376	0.50182	0.0090665	150.96	−0.0035421	0.0050017
1499.9	0.014806	0.060946	0.99720	35.588	−0.043959	0.035511
341.95	0.072705	0.024435	1	11.168	−0.10975	0.14282
94.680	0.25263			3.9020	0.18740	0.33862
29.735	0.49324			1.3818	0.64670	0.45158
10.006	0.31317			0.46663	0.30606	0.27327
0.048900	1					

TABLE VI: Molecular GTO basis set used for the sodium atoms.

For non-sigma states there is an important magnetic hyperfine effect due to the interaction between the electronic orbital motion and the nuclear magnetic moments. As we consider only $^3\Sigma$ electronic states, this effect falls outside the scope of the present investigation.

Appendix A: The STO/N21-own basis set for Na_2

The basis set used for sodium is reported in Table VI. This basis set is heavily inspired by the STO-6G and N21 basis sets, modified to give an accurate atomic Fermi contact parameter.

[1] R. A. Frosch and H. M. Foley, Phys. Rev. **88**, 1337 (1952).

[2] J. Aldegunde, B. A. Rivington, P. S. Żuchowski, and J. M. Hutson, Phys. Rev. A **78**, 033434 (2008).

[3] J. Aldegunde and J. M. Hutson, Phys. Rev. A **79**, 013401 (2009).

[4] P. Kristiansen and L. Veseth, J. Chem. Phys. **84**, 2711 (1986).

[5] P. Kristiansen and L. Veseth, J. Chem. Phys. **84**, 6336 (1986).

[6] D. P. Chong, S. R. Langhoff, and J. Charles W. Bauschlicher, The Journal of Chemical Physics **94**, 3700 (1991).

[7] I. Carmichael, The Journal of Physical Chemistry **94**, 5734 (1990), http://pubs.acs.org/doi/pdf/10.1021/j100378a025.

[8] R. Prasad, The Journal of Chemical Physics **120**, 10089 (2004).

[9] M. Mladenović, M. Perić, and B. Engels, The Journal of Chemical Physics **122**, 144306 (2005).

[10] H. M. Quiney and P. Belanzoni, Chemical Physics Letters **353**, 253 (2002).

[11] J. A. J. Fitzpatrick, F. R. Manby, and C. M. Western, The Journal of Chemical Physics **122**, 084312 (2005).

[12] T. Takekoshi, C. Strauss, F. Lang, J. H. Denschlag, M. Lysebo, and L. Veseth, Phys. Rev. A **83**, 062504 (2011).

[13] M. Lysebo and L. Veseth, Phys. Rev. A **79**, 062704 (2009).

[14] T. Helgaker, P. Jørgensen, and J. Olsen, *Molecular Electronic Structure Theory* (John Wiley & Sons, LTD, Chichester, 2000).

[15] E. Arimondo, M. Inguscio, and P. Violino, Reviews of Modern Physics **49**, 31 (1977).

[16] M. Larsson, Physica Scripta **23**, 835 (1981).

[17] E. Wigner and E. Witmer, Z. Phys. **51**, 859 (1928).

[18] M. W. Schmidt, K. K. Baldridge, J. A. Boatz, S. T. Elbert, M. S. Gordon, J. H. Jensen, S. Koseki, N. Matsunaga, K. A. Nguyen, S. Su, T. L. Windus, M. Dupuis, and J. A. Montgomery, Journal of Computational Chemistry **14**, 1347 (1993).

[19] M. S. Gordon and M. W. Schmidt, "Advances in electronic structure theory: GAMESS a decade later," in *Theory and Applications of Computational Chemistry: the first forty years*, edited by C. E. Dykstra, G. Frenking, K. S. Kim, and G. E. Scuseria (Elsevier, Amsterdam, 2005) pp. 1167–1189.

[20] W. J. Hehre, R. F. Stewart, and J. A. Pople, J. Chem. Phys. **51**, 2657 (1969).

[21] B. Minaev, Spectrochimica Acta Part A **62**, 790 (2005).

[22] D. D. Konowalow and J. L. Fish, Chemical Physics **84**, 463 (1984).

[23] S. Magnier, P. MilliÃ©, O. Dulieu, and F. MasnouSeeuws, J. Chem. Phys. **98**, 7113 (1993).

[24] S. Magnier and P. Millié, Phys. Rev. A **54**, 204 (1996).

[25] S. J. Park, S. W. Suh, Y. S. Lee, and G.-H. Jeung, Journal of Molecular Spectroscopy **207**, 129 (2001).

[26] B. O. Roos, "The complete active space self-consistent field method and its applications in electronic structure calculations," in *Advances in Chemical Physics* (John Wiley & Sons, Inc., 2007) pp. 399–445.

[27] *GAMESS User's Guide*, Department of Chemistry, Iowa State University, Ames, IA 50011 (2012).

[28] B. R. Brooks and H. F. Schaefer, J. Chem. Phys **70**, 5092 (1979).

[29] G. Chaban, M. W. Schmidt, and M. S. Gordon, Theor. Chem. Acc. **97**, 88 (1997).

[30] J. Emsley, *The Elements, Oxford Chemistry Guides* (Oxford Univ. Press, New York, NY, 1995).

[31] H. E. Radford, Phys. Rev. **136**, A1571 (1964).